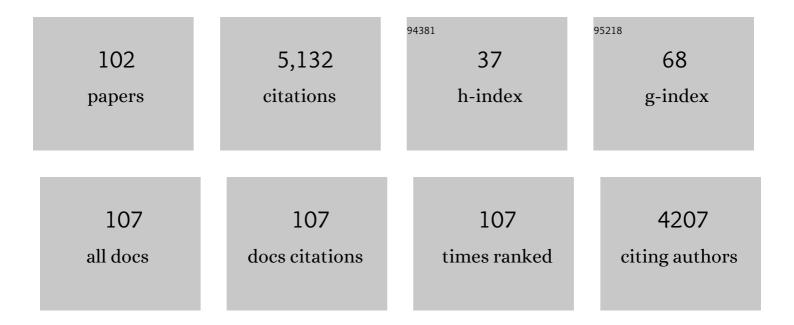
Joseph A Resing

List of Publications by Year in descending order

Source: https://exaly.com/author-pdf/5905530/publications.pdf

Version: 2024-02-01



#	Article	IF	CITATIONS
1	Basin-scale transport of hydrothermal dissolved metals across the South Pacific Ocean. Nature, 2015, 523, 200-203.	13.7	397
2	The GEOTRACES Intermediate Data Product 2017. Chemical Geology, 2018, 493, 210-223.	1.4	257
3	Evolution of a Submarine Magmatic-Hydrothermal System: Brothers Volcano, Southern Kermadec Arc, New Zealand. Economic Geology, 2005, 100, 1097-1133.	1.8	250
4	Determination of iron in seawater by flow injection analysis using in-line preconcentration and spectrophotometric detection. Marine Chemistry, 1995, 50, 3-12.	0.9	186
5	Calculation of lava effusion rates from Landsat TM data. Bulletin of Volcanology, 1998, 60, 52-71.	1.1	168
6	Aerosol iron and aluminum solubility in the northwest Pacific Ocean: Results from the 2002 IOC cruise. Geochemistry, Geophysics, Geosystems, 2006, 7, n/a-n/a.	1.0	167
7	Active submarine eruption of boninite in the northeastern Lau Basin. Nature Geoscience, 2011, 4, 799-806.	5.4	163
8	Long-term eruptive activity at a submarine arc volcano. Nature, 2006, 441, 494-497.	13.7	141
9	Submarine venting of liquid carbon dioxide on a Mariana Arc volcano. Geochemistry, Geophysics, Geosystems, 2006, 7, n/a-n/a.	1.0	139
10	The solubility and deposition of aerosol Fe and other trace elements in the North Atlantic Ocean: Observations from the A16N CLIVAR/CO2 repeat hydrography section. Marine Chemistry, 2010, 120, 57-70.	0.9	126
11	Fluorometric Determination of Al in Seawater by Flow Injection Analysis with In-Line Preconcentration. Analytical Chemistry, 1994, 66, 4105-4111.	3.2	122
12	Determination of manganese in seawater using flow injection analysis with on-line preconcentration and spectrophotometric detection. Analytical Chemistry, 1992, 64, 2682-2687.	3.2	112
13	Hydrothermal activity and volcano distribution along the Mariana arc. Journal of Geophysical Research, 2008, 113, .	3.3	107
14	Opposing trends in crustal thickness and spreading rate along the back-arc Eastern Lau Spreading Center: Implications for controls on ridge morphology, faulting, and hydrothermal activity. Earth and Planetary Science Letters, 2006, 245, 655-672.	1.8	97
15	Submarine hydrothermal activity along the midâ€Kermadec Arc, New Zealand: Largeâ€scale effects on venting. Geochemistry, Geophysics, Geosystems, 2007, 8, .	1.0	97
16	How many vent fields? New estimates of vent field populations on ocean ridges from precise mapping of hydrothermal discharge locations. Earth and Planetary Science Letters, 2016, 449, 186-196.	1.8	92
17	Pacific Ocean aerosols: Deposition and solubility of iron, aluminum, and other trace elements. Marine Chemistry, 2013, 157, 117-130.	0.9	89
18	High SO2 flux, sulfur accumulation, and gas fractionation at an erupting submarine volcano. Geology, 2011, 39, 803-806.	2.0	87

#	Article	IF	CITATIONS
19	Particle size and aerosol iron solubility: A high-resolution analysis of Atlantic aerosols. Marine Chemistry, 2010, 120, 14-24.	0.9	81
20	Hydrothermal plumes along the East Pacific Rise, 8°40′ to 11°50′N: Plume distribution and relationship to the apparent magmatic budget. Earth and Planetary Science Letters, 1994, 128, 1-17.	1.8	78
21	Western Pacific coastal sources of iron, manganese, and aluminum to the Equatorial Undercurrent. Global Biogeochemical Cycles, 2010, 24, .	1.9	78
22	Venting of Acid-Sulfate Fluids in a High-Sulfidation Setting at NW Rota-1 Submarine Volcano on the Mariana Arc. Economic Geology, 2007, 102, 1047-1061.	1.8	76
23	Analytical intercomparison results from the 1990 Intergovernmental Oceanographic Commission open-ocean baseline survey for trace metals: Atlantic Ocean. Marine Chemistry, 1995, 49, 253-265.	0.9	75
24	Exploring the Submarine Ring of Fire: Mariana Arc - Western Pacific. Oceanography, 2007, 20, 68-79.	0.5	75
25	Manganese and methane in hydrothermal plumes along the East Pacific Rise, 8°40′ to 11°50′N. Geochim Et Cosmochimica Acta, 1995, 59, 4147-4165.	ica 1.6	62
26	CO2 and 3He in hydrothermal plumes: implications for mid-ocean ridge CO2 flux. Earth and Planetary Science Letters, 2004, 226, 449-464.	1.8	62
27	Chemistry of hydrothermal plumes above submarine volcanoes of the Mariana Arc. Geochemistry, Geophysics, Geosystems, 2009, 10, .	1.0	62
28	Explorations of Mariana Arc volcanoes reveal new hydrothermal systems. Eos, 2004, 85, 37.	0.1	58
29	Manganese and iron in hydrothermal plumes resulting from the 1996 Gorda Ridge Event. Deep-Sea Research Part II: Topical Studies in Oceanography, 1998, 45, 2683-2712.	0.6	54
30	A dissolved cobalt plume in the oxygen minimum zone of the eastern tropical South Pacific. Biogeosciences, 2016, 13, 5697-5717.	1.3	52
31	Helium isotope, <scp>C</scp> / ³ <scp>H</scp> e, and <scp>B</scp> aâ€ <scp>N</scp> bâ€ <scp>T</scp> i signatures in the northern <scp>L</scp> au <scp>B</scp> asin: Distinguishing arc, backâ€arc, and hotspot affinities. Geochemistry, Geophysics, Geosystems. 2015. 16, 1133-1155.	1.0	50
32	Chemical and physical diversity of hydrothermal plumes along the East Pacific Rise, 8°45′N to 11°50′N. Geophysical Research Letters, 1993, 20, 2913-2916.	1.5	48
33	Multiple hydrothermal sources along the south Tonga arc and Valu Fa Ridge. Geochemistry, Geophysics, Geosystems, 2007, 8, .	1.0	46
34	Hydrothermal venting along Earth's fastest spreading center: East Pacific Rise, 27.5°-32.3°. Journal of Geophysical Research, 2002, 107, EPM 2-1-EPM 2-14.	3.3	42
35	Hydrothermal exploration of the Fonualei Rift and Spreading Center and the Northeast Lau Spreading Center. Geochemistry, Geophysics, Geosystems, 2006, 7, n/a-n/a.	1.0	41
36	Abundant hydrothermal venting along melt-rich and melt-free ridge segments in the Lau back-arc basin. Geophysical Research Letters, 2006, 33, .	1.5	40

#	Article	IF	CITATIONS
37	Aeolian Contamination of Se and Ag in the North Pacific from Asian Fossil Fuel Combustion. Environmental Science & Technology, 2010, 44, 1587-1593.	4.6	40
38	Radium-228 as a tracer of dissolved trace element inputs from the Peruvian continental margin. Marine Chemistry, 2018, 201, 20-34.	0.9	39
39	Unique event plumes from a 2008 eruption on the Northeast Lau Spreading Center. Geochemistry, Geophysics, Geosystems, 2011, 12, n/a-n/a.	1.0	37
40	Methods for analyzing the concentration and speciation of major and trace elements in marine particles. Progress in Oceanography, 2015, 133, 32-42.	1.5	37
41	Eruptionâ€fed particle plumes and volcaniclastic deposits at a submarine volcano: NW Rotaâ€1, Mariana Arc. Journal of Geophysical Research, 2008, 113, .	3.3	36
42	Dissolved Fe and Al in the upper 1000 m of the eastern Indian Ocean: A highâ€resolution transect along 95°E from the Antarctic margin to the Bay of Bengal. Global Biogeochemical Cycles, 2015, 29, 375-396.	1.9	36
43	Significant discharge of CO2 from hydrothermalism associated with the submarine volcano of El Hierro Island. Scientific Reports, 2016, 6, 25686.	1.6	35
44	Impact of hydrothermalism on the ocean iron cycle. Philosophical Transactions Series A, Mathematical, Physical, and Engineering Sciences, 2016, 374, 20150291.	1.6	35
45	Submarine Magmatic-Hydrothermal Systems at the Monowai Volcanic Center, Kermadec Arc. Economic Geology, 2012, 107, 1669-1694.	1.8	33
46	Lavaâ€seawater interactions at shallowâ€water submarine lava flows. Geophysical Research Letters, 1991, 18, 1731-1734.	1.5	32
47	Understanding a submarine eruption through time series hydrothermal plume sampling of dissolved and particulate constituents: <scp>W</scp> est <scp>M</scp> ata, 2008–2012. Geochemistry, Geophysics, Geosystems, 2014, 15, 4631-4650.	1.0	31
48	Highâ€resolution surveys along the hot spot–affected Galápagos Spreading Center: 2. Influence of magma supply on volcanic morphology. Geochemistry, Geophysics, Geosystems, 2008, 9, .	1.0	30
49	Catalytically enhanced spectrophotometric determination of manganese in seawater by flow-injection analysis with a commercially available resin for on-line preconcentration. Limnology and Oceanography: Methods, 2006, 4, 105-113.	1.0	27
50	Hydrothermal cooling along the Eastern Lau Spreading Center: No evidence for discharge beyond the neovolcanic zone. Geochemistry, Geophysics, Geosystems, 2010, 11, .	1.0	26
51	The trace element composition of suspended particulate matter in the upper 1000m of the eastern North Atlantic Ocean: A16N. Marine Chemistry, 2012, 142-144, 41-53.	0.9	26
52	Eruptive modes and hiatus of volcanism at West Mata seamount, NE Lau basin: 1996-2012. Geochemistry, Geophysics, Geosystems, 2014, 15, 4093-4115.	1.0	26
53	Hydrography and geochemistry of sea surface hydrothermal plumes resulting from Hawaiian coastal volcanism. Journal of Geophysical Research, 1995, 100, 13555.	3.3	25
54	Geochemistry of atmospheric aerosols generated from lava-seawater interactions. Geophysical Research Letters, 2002, 29, 49-1-49-4.	1.5	25

#	Article	IF	CITATIONS
55	Imaging of CO ₂ bubble plumes above an erupting submarine volcano, NW Rotaâ€1, Mariana Arc. Geochemistry, Geophysics, Geosystems, 2014, 15, 4325-4342.	1.0	25
56	Seasonal and spatial variabilities in northern Gulf of Alaska surface water iron concentrations driven by shelf sediment resuspension, glacial meltwater, a Yakutat eddy, and dust. Global Biogeochemical Cycles, 2017, 31, 942-960.	1.9	25
57	Geological interpretation of volcanism and segmentation of the <scp>M</scp> ariana backâ€arc spreading center between 12.7° <scp>N</scp> and 18.3° <scp>N</scp> . Geochemistry, Geophysics, Geosystems, 2017, 18, 2240-2274.	1.0	25
58	Chemical plumes from low-temperature hydrothermal venting on the eastern flank of the Juan de Fuca Ridge. Journal of Geophysical Research, 1997, 102, 15433-15446.	3.3	24
59	Particulate iron, aluminum, and manganese in the Pacific equatorial undercurrent and low latitude western boundary current sources. Marine Chemistry, 2012, 142-144, 54-67.	0.9	24
60	The impact of circulation and dust deposition in controlling the distributions of dissolved Fe and Al in the south Indian subtropical gyre. Marine Chemistry, 2015, 176, 110-125.	0.9	24
61	The chemistry of lava–seawater interactions: the generation of acidity. Geochimica Et Cosmochimica Acta, 1999, 63, 2183-2198.	1.6	23
62	Variations in hydrothermal methane and hydrogen concentrations following the 1998 eruption at Axial Volcano. Geophysical Research Letters, 1999, 26, 3453-3456.	1.5	23
63	Highâ€resolution surveys along the hot spot–affected Gálapagos Spreading Center: 3. Black smoker discoveries and the implications for geological controls on hydrothermal activity. Geochemistry, Geophysics, Geosystems, 2008, 9, .	1.0	22
64	A Recent Volcanic Eruption Discovered on the Central Mariana Back-Arc Spreading Center. Frontiers in Earth Science, 2018, 6, .	0.8	22
65	The water-column chemical signature after the 1998 Eruption of Axial Volcano. Geophysical Research Letters, 1999, 26, 3645-3648.	1.5	21
66	Decay of hydrothermal output following the 1998 seafloor eruption at Axial Volcano: Observations and models. Journal of Geophysical Research, 2004, 109, .	3.3	21
67	Highâ€resolution surveys along the hot spot–affected Galápagos Spreading Center: 1. Distribution of hydrothermal activity. Geochemistry, Geophysics, Geosystems, 2008, 9, .	1.0	21
68	Evidence for iron and sulfur enrichments in hydrothermal plumes at Axial Volcano following the January-February 1998 eruption. Geophysical Research Letters, 1999, 26, 3649-3652.	1.5	20
69	Tectonic/volcanic segmentation and controls on hydrothermal venting along Earth's fastest seafloor spreading system, EPR 27°-32°S. Geochemistry, Geophysics, Geosystems, 2004, 5, n/a-n/a.	1.0	20
70	Calcium carbonate dissolution in the upper 1000 m of the eastern North Atlantic. Global Biogeochemical Cycles, 2014, 28, 386-397.	1.9	19
71	Developing Autonomous Observing Systems for Micronutrient Trace Metals. Frontiers in Marine Science, 2019, 6, .	1.2	19
72	The chemistry of lava-seawater interactions II: the elemental signature. Geochimica Et Cosmochimica Acta, 2002, 66, 1925-1941.	1.6	18

#	Article	IF	CITATIONS
73	First hydrothermal discoveries on the <scp>A</scp> ustralianâ€ <scp>A</scp> ntarctic <scp>R</scp> idge: Discharge sites, plume chemistry, and vent organisms. Geochemistry, Geophysics, Geosystems, 2015, 16, 3061-3075.	1.0	18
74	The NE Lau Basin: Widespread and Abundant Hydrothermal Venting in the Back-Arc Region Behind a Superfast Subduction Zone. Frontiers in Marine Science, 2019, 6, .	1.2	18
75	The Solomon Sea: its circulation, chemistry, geochemistry and biology explored during two oceanographic cruises. Elementa, 2017, 5, .	1.1	17
76	Methane dynamics in hydrothermal plumes over a superfast spreading center: East Pacific Rise, 27.5°–32.3°S. Journal of Geophysical Research, 2005, 110, .	3.3	15
77	The Effect of Arc Proximity on Hydrothermal Activity Along Spreading Centers: New Evidence From the Mariana Back Arc (12.7°N–18.3°N). Geochemistry, Geophysics, Geosystems, 2017, 18, 4211-4228.	1.0	15
78	Trace element composition of suspended particulate matter along three meridional CLIVAR sections in the Indian and Southern Oceans: Impact of scavenging on Al distributions. Chemical Geology, 2018, 502, 15-28.	1.4	15
79	Processes controlling the distribution of dissolved Al and Ga along the U.S. GEOTRACES East Pacific Zonal Transect (GP16). Deep-Sea Research Part I: Oceanographic Research Papers, 2019, 147, 128-145.	0.6	15
80	Atmospheric deposition of glacial iron in the Gulf of Alaska impacted by the position of the Aleutian Low. Geophysical Research Letters, 2017, 44, 5053-5061.	1.5	14
81	Chemical Fluxes From a Recently Erupted Shallow Submarine Volcano on the Mariana Arc. Geochemistry, Geophysics, Geosystems, 2018, 19, 1660-1673.	1.0	13
82	Changes in the distribution of Al and particulate Fe along A16N in the eastern North Atlantic Ocean between 2003 and 2013: Implications for changes in dust deposition. Marine Chemistry, 2015, 177, 57-68.	0.9	12
83	Al and pH anomalies in the Manus Basin reappraised: comments on the paper by T. Gamo et al., "Hydrothermal plumes in the eastern Manus Basin, Bismarck Sea: CH4, Mn, Al and pH anomalies― Deep-Sea Research Part I: Oceanographic Research Papers, 1996, 43, 1867-1872.	0.6	10
84	Hydrothermal activity in the Northwest Lau Backarc Basin: Evidence from water column measurements. Geochemistry, Geophysics, Geosystems, 2012, 13, .	1.0	10
85	Quantifying the Impact of Atmospheric Deposition on the Biogeochemistry of Fe and Al in the Upper Ocean: A Decade of Collaboration with the US CLIVAR-CO2 Repeat Hydrography Program. Oceanography, 2014, 27, 62-65.	0.5	10
86	Posteruption Enhancement of Hydrothermal Activity: A 33‥ear, Multieruption Time Series at Axial Seamount (Juan de Fuca Ridge). Geochemistry, Geophysics, Geosystems, 2019, 20, 814-828.	1.0	9
87	Hydrothermal Activity and Seismicity at Teahitia Seamount: Reactivation of the Society Islands Hotspot?. Frontiers in Marine Science, 2020, 7, .	1.2	9
88	Methane, manganese, and helium in hydrothermal plumes following volcanic eruptions on the East Pacific Rise near 9°50′N. Geochemistry, Geophysics, Geosystems, 2008, 9, .	1.0	8
89	Extensive hydrothermal activity revealed by multi-tracer survey in the Wallis and Futuna region (SW) Tj ETQq1	1 0.784314 0.6	l rgBT /Over
90	The characteristics of Fe speciation and Fe-binding ligands in the Mariana back-arc hydrothermal plumes. Geochimica Et Cosmochimica Acta, 2021, 292, 24-36.	1.6	8

#	Article	IF	CITATIONS
91	Dissolved Gas and Metal Composition of Hydrothermal Plumes From a 2008 Submarine Eruption on the Northeast Lau Spreading Center. Frontiers in Marine Science, 2020, 7, .	1.2	7
92	Hydroacoustics of a submarine eruption in the Northeast Lau Basin using an acoustic glider. , 2010, , .		6
93	Patterns of Fine Ash Dispersal Related to Volcanic Activity at West Mata Volcano, NE Lau Basin. Frontiers in Marine Science, 2019, 6, .	1.2	4
94	Spotlight: Northwest Rota-1 Seamount. Oceanography, 2010, 23, 182-183.	0.5	3
95	Hunting for Hydrothermal Vents Along the Galápagos Spreading Center. Oceanography, 2007, 20, 100-107.	0.5	2
96	Energy dispersive Xâ€ray fluorescence methodology and analysis of suspended particulate matter in seawater for trace element compositions and an intercomparison with highâ€resolution inductively coupled plasmaâ€mass spectrometry. Limnology and Oceanography: Methods, 2021, 19, 401-415.	1.0	2
97	Constraining the Contribution of Hydrothermal Iron to Southern Ocean Export Production Using Deep Ocean Iron Observations. Frontiers in Marine Science, 2022, 9, .	1.2	2
98	The water-column chemical signature after the 1998 eruption of Axial Volcano. Geophysical Research Letters, 1999, 26, 3645-3648.	1.5	1
99	LA DIFFÉRENCIATION PSYCHOLOGIQUE ET LES FORMES DE LA PATHOLOGIE. Applied Psychology, 1965, 14, 62-64.	4.4	0
100	Fingerprints of a trace nutrient. Nature, 2014, 511, 164-165.	13.7	0
101	Organic Biogeochemistry in West Mata, NE Lau Hydrothermal Vent Fields. Geochemistry, Geophysics, Geosystems, 2021, 22, e2020GC009481.	1.0	0
102	Constraining the Solomon Sea as a source of Al and Mn to the Equatorial Undercurrent. Deep-Sea Research Part I: Oceanographic Research Papers, 2021, 174, 103559.	0.6	0